Since January 2020 Elsevier has created a COVID-19 resource centre with free information in English and Mandarin on the novel coronavirus COVID-19. The COVID-19 resource centre is hosted on Elsevier Connect, the company's public news and information website.

Available online at www.sciencedirect.com
SCIENCE DIRECT®
Virology 318 (2004) 381–392
VIROLOGY
www.elsevier.com/locate/yviro

Differential regulation of innate and adaptive immune responses in viral encephalitis

Julia D. Rempel,[a,b] Shannon J. Murray,[a] Jeffrey Meisner,[a] and Michael J. Buchmeier[a,*]

[a] *Division of Virology, Department of Neuropharmacology, The Scripps Research Institute, La Jolla, CA 92037, USA*
[b] *Liver Diseases Unit, Department of Medicine, University of Manitoba Winnipeg, Manitoba, Canada R3E 3P4*

Received 24 February 2003; returned to author for revision 22 August 2003; accepted 9 September 2003

Abstract

Viral encephalitis is a global health concern. The ability of a virus to modulate the immune response can have a pivotal effect on the course of disease and the fate of the infected host. In this study, we sought to understand the immunological basis for the fatal encephalitis following infection with the murine coronavirus, mouse hepatitis virus (MHV)-JHM, in contrast with the more attenuated MHV-A59. Distinct glial cell cytokine and chemokine response patterns were observed within 3 days after infection, became progressively more polarized during the course of infection and with the infiltration of leukocytes. In the brain, MHV-JHM infection induced strong accumulation of IFNβ mRNA relative to IFNγ mRNA. This trend was reversed in MHV-A59 infection and was accompanied by increased CD8 T cell infiltration into brain compared to MHV-JHM infection. Increased apoptosis appeared to contribute to the diminished presence of CD8 T cells in MHV-JHM-infected brain with the consequence of a lower potential for IFNγ production and antiviral activity. MHV-JHM infection also induced sustained mRNA accumulation of the innate immune response products interleukin (IL)-6 and IL-1. Furthermore, high levels of macrophage-inflammatory protein (MIP)-1α, MIP-1β, and MIP-2 mRNA were observed at the onset of MHV-JHM infection and correlated with a marked elevation in the number of macrophages in the brain on day 7 compared to MHV-A59 infection. These observations indicate that differences in the severity of viral encephalitis may reflect the differential ability of viruses to stimulate innate immune responses within the CNS and subsequently the character of infiltrating leukocyte populations.

Keywords: Neuroimmunology; Viral; Cytokines; Chemokines; T Lymphocytes

Introduction

The impact of emerging and reemerging viral induced encephalitis is being felt globally (Shoji et al., 2002). The outcome of viral encephalitis can be considered the result of a competition between the virus and the host immune system. The parameters governing this outcome include the intrinsic virulence of the infecting virus, its tropism, replicative potential, and interactions with the immune system. In addition, the virus infection triggers a host immune response which may be protective or may contribute to the disease process (reviewed in (Noseworthy, 1999; Pavesi et al., 1992)). Thus, the balance of these factors within the CNS may result in a return to homeostasis, the development of autoimmunity, or the occurrence of fatal encephalitis.

A variety of murine coronavirus strains differ radically in their pathogenic potential and disease outcome rendering them useful models to study the generation of immune responses critical to this balance. Infection with the mouse hepatitis virus (MHV)-JHM causes severe encephalitis with a high mortality when inoculated intracranially or intranasally into susceptible adult mice (Phillips et al., 1999). In contrast, infection with the mildly neurovirulent MHV-A59 strain results in viral clearance and the development of demyelinating lesions resembling those in multiple sclerosis (Lai and Stohlman, 1981; Lavi et al., 1984; Woyciechowska et al., 1984; Zou et al., 1999). Although these viruses share many features, differences in the spike glycoprotein, hemagglutinin/esterase, and other proteins may be responsible for the enhanced capacity of MHV-JHM to infect the brain.

Abbreviations: MHV, mouse hepatitis virus; MIF, macrophage migration inhibitory factor; MIP, macrophage-inflammatory protein.

* Corresponding author. Division of Virology, Department of Neuropharmacology, The Scripps Research Institute, Maildrop CVN-8, 10550 North Torrey Pines Road, La Jolla, CA 92037. Fax: +1-858-784-7162.
E-mail address: buchm@scripps.edu (M.J. Buchmeier).

0042-6822/$ - see front matter © 2003 Elsevier Inc. All rights reserved.
doi:10.1016/j.virol.2003.09.023

Despite observations from different laboratories which suggest that MHV-JHM and MHV-A59 are able to infect astrocytes, oligodendrocytes, and to a lesser degree neurons, MHV-JHM invades the brain more extensively (Lavi et al., 1999; Phillips et al., 2002; van Berlo et al., 1989; Woyciechowska et al., 1984). Variation is also apparent in the CD8 T cell epitopes, such that of the two known epitopes on the MHV-JHM spike protein (S510 and S598), only one (S598) is shared by MHV-A59 due to a deletion in the MHV-A59 spike protein (Bergmann et al., 1996; Castro and Perlman, 1996). In addition, it has been speculated that MHV-A59 may contain unidentified CD8 epitopes (Marten et al., 2001).

It is now appreciated that glial and neuronal cells are capable of responding to infection by releasing chemokines and cytokines that trigger innate immune responses in the absence of peripheral immune cells (Olson et al., 2001). Release of type I (IFNα/β) and type II (IFNγ) interferons and production of pro-inflammatory cytokines such as interleukin (IL)-6 and IL-1 are important early events in response to viral infection (Parra et al., 1997; LeBlanc et al., 1999). IFNγ, in particular, is critical in resolving MHV infection (Marten et al., 2001; Parra et al., 1999; Schijns et al., 1998). The production of innate immune mediators, such as IL-12, IL-4, and interferons, acts to establish a microenvironment capable of directing adaptive T and B cell responses; whereas, production of RANTES, macrophage-inflammatory protein (MIP), and other chemokines acts to recruit T cells and macrophages into the CNS following infection (Lane et al., 1998; Liu and Lane, 2001). This migration in response to chemokines is reenforced later by the infiltrating leukocytes themselves. These cells can provide protective immunity against CNS infections, as demonstrated by the requirement of cytolytic CD8 T cell activity in the clearance of MHV infections (Bergmann et al., 1999; Gombold et al., 1995; Marten et al., 2001). However, an inappropriate combination of these same factors or timing of their release may result in the initiation of neurologic disease (Olsson, 1995). Thus, the quality and magnitude of the innate and adaptive responses can influence both the recovery from infection and the development of immunopathology.

Much attention has been given to understanding how immune responses participate in demyelinating disease. In this study, we sought to understand how viral modulation of early immune responses might influence the outcome of CNS disease following infection with the highly neurovirulent virus, MHV-JHM. MHV-JHM was administered intracranially in the absence of immune manipulation resulting in fatal encephalomyelitis. Chemokine, cytokine, and cellular immune responses in the CNS compartment were documented and compared against mildly neurovirulent MHV-A59 infection. The lack of MHV-JHM clearance was associated with diminished IFNγ and CD8 T cell responses. However, the expression of IL-6 and IFNβ mRNA was unabated. In contrast, mice infected with MHV-A59 exhibited decreasing accumulation of IL-6 and IFNβ mRNA, combined with early and consistent IFNγ transcripts that corresponded with the influx of CD8 T cells into the CNS, and control of viral replication by 7 days after infection. Furthermore, MHV-JHM infection was marked by high levels of MIP-1α, MIP-1β, and MIP-2 mRNA correlating with a greater infiltration of macrophages into the brain compared to that observed in MHV-A59-infected animals. The data presented in this report highlight the crucial role that viral induction of early innate immune responses may have in outcome of disease within the CNS.

Results

Viral titers and disease severity

To better understand how immune responses elicited by a virus might contribute to fatal encephalitis, C57Bl/6 mice were injected intracranially with MHV-JHM or the control virus MHV-A59. The viral burden within the brain was assessed on days 3, 5, and 7 after inoculation. MHV-JHM

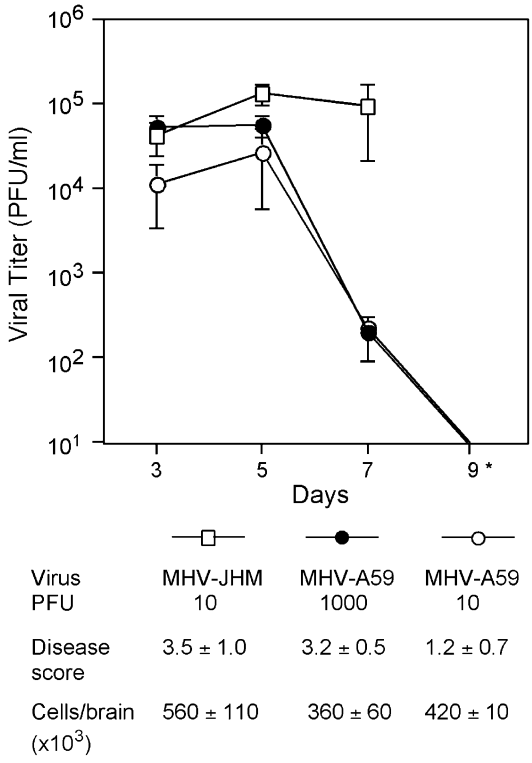

Fig. 1. Viral titers and disease scores. Mice were infected with MHV-JHM and MHV-A59 at doses indicated. Brain viral titers were determined by plaque assay. *By day 9, mice infected with MHV-JHM generally had succumbed to infection, whereas replicating virus was not detected in MHV-A59-infected brains. Mean PFU/ml ± SE are shown ($n = 4–8$ mice per group). Disease scores were assessed on day 7, the peak of acute encephalitis ($n = 15$ mice/group). On day 7, cells were isolated from infected brains as described in Materials and Methods. Live cells were identified by trypan blue dye exclusion.

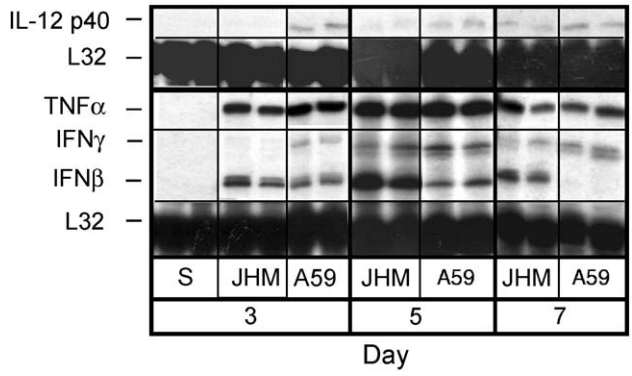

Fig. 2. MHV-JHM infection induces sustained accumulation of IFNβ mRNA. Mice were infected intracranially with MHV-JHM, control virus, and saline. On days 3, 5, and 7 p.i, animals were perfused and brains were harvested. Total RNA was extracted and analyzed by RPA. "S" indicates saline-injected mice. Two representative samples shown from four experiments. Mean band densities were calculated using NIH Image 1.161 software reflective of signal intensity. Band densities for IFNγ and IFNβ were normalized against corresponding L32 (housekeeping) band densities and averaged. To compare the relative difference in IFNβ and IFNγ mRNA accumulation, the average band densities were expressed as ratios.

infections resulted in high viral titers within the CNS that remained elevated (Fig. 1). In contrast, following MHV-A59 infection, initially high titers on day 5 were reduced by day 7 and undetectable by day 9.

Disease was scored on day 7, at the peak of encephalitis for both viruses. At equivalent doses of 10 PFU, MHV-JHM infection resulted in considerably more severe disease than MHV-A59 (scores of 3.5 ± 1.0 vs. 1.2 ± 0.7, respectively; Fig. 1). MHV-A59 needed to be given at 1000 PFU to induce similar disease scores on day 7 as MHV-JHM at 10 PFU. Therefore, MHV-A59 was also used at 1000 PFU to provide a control that more closely approximated the severity of clinical disease seen in MHV-JHM infection. Examining immune responses from viral infections resulting in similar disease scores increased our confidence that the responses measured following MHV-JHM infection were a function of viral activity and not merely secondary to the more severe clinical disease seen in MHV-JHM infection.

Mononuclear cells were isolated from infected brains and the total number of infiltrating immune cells was estimated. The numbers of inflammatory cells isolated from MHV-JHM-infected brains were equivalent or slightly higher than

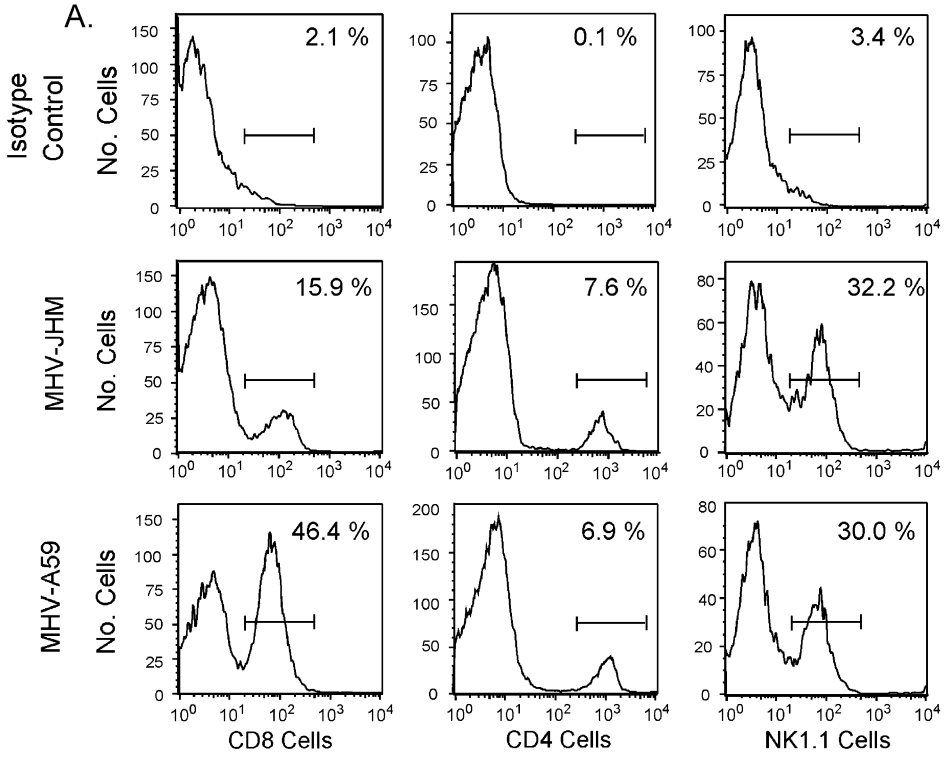

B.

Cells	N	MHV-JHM	MHV-A59	*p* value
CD8	10	13.6 ± 1.5	32.8 ± 3.4	< 0.001
CD4	4	6.2 ± 0.7	7.2 ± 0.5	> 0.05
NK	4	32.1 ± 9.0	30.6 ± 5.2	> 0.05

Fig. 3. Diminished CD8 T cell infiltration following MHV-JHM infection. Mice were inoculated with MHV-JHM and MHV-A59. On day 7, mononuclear cells were isolated from infected brains and stained for either anti-CD8, anti-CD4, or anti-NK1.1, and analyzed by FACS analysis. (A) One representative experiment for each of anti-CD8, anti-CD4, or anti-NK1.1 staining is shown. (B) Means ± SE for 4–6 mice/*N* experiments is shown.

the number of cells from MHV-A59-infected brains, independent of the MHV-A59 dose (Fig. 1). This indicated that the high mortality among MHV-JHM infected mice was not due to a failure to induce mononuclear cell infiltration into the CNS.

MHV-JHM infection induces enhanced IFNβ and reduced IFNγ transcript levels

The nature of the immune response induced by MHV-JHM infection was evaluated by examining cytokine mRNA levels in whole brain. Mice were injected with MHV-JHM, MHV-A59, or saline (sham). Total RNA was isolated from brains harvested on days 3, 5, and 7 postinjection. With the exception of IL-18 and transforming growth factor (TGF)-β, which were consistently elevated from background even in uninoculated brain (data not shown), saline injections did not induce detectable levels of mRNA message for the cytokines examined (Fig. 2). Macrophage migration inhibitory factor (MIF) (data not shown) and tumor neurosis factor (TNF)-α (Fig. 2) mRNA transcripts were strongly and similarly enhanced in both MHV-JHM and MHV-A59 infections.

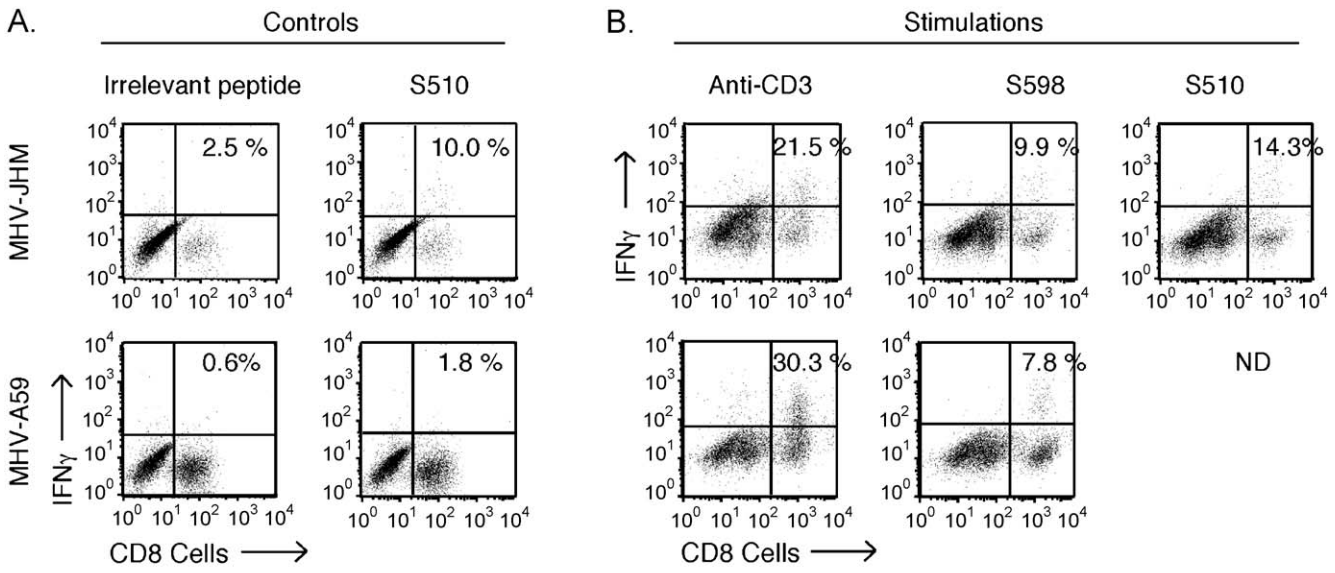

	MHV-JHM	MHV-A59	
C. % IFNγ+ CD8 cells:			
Anti-CD3:	21.5 ± 3.4	30.3 ± 2.7	
Sum of viral : (S510 and S598)	24.2 ± 2.0	8.9 ± 0.9	
Viral/anti-CD3:	1.1	0.29	
D. % IFNγ+ total cells : (Anti-CD3)	2.8 ± 0.4	7.3 ± 1.1	$p < 0.05$

Fig. 4. MHV-JHM infection results in reduced IFNγ production within the CNS. Cells isolated from infected brains were stimulated with viral peptides or anti-CD3 in the presence of brefeldin A (mean percents ± SE shown reflect 4–6 mice per five experiments). Cells were stained for the detection of CD8 and IFNγ. (A) Stimulation with S510 peptide, following MHV-A59 infection, and an irrelevant peptide, following both infections, results in negligible amounts of IFNγ+ cells. Percentages depict the IFNγ+ CD8 cells in the upper right-hand quadrant from one representative experiment. These negative controls were not run every experiment due to the number of cells isolated from brains. (B) Mean percentages are shown and are represented by the IFNγ+ CD8 cells in the upper right-hand quadrants of the graphs. (C) The percentage of IFNγ+ CD8 cells following viral peptide stimulation was normalized against the percentage of IFNγ+ CD8 cells following anti-CD3 stimulation, for example, 24.2/21.5 = 1.1. (D) The percentage of IFNγ+ total cells within the mononuclear gate was determined following anti-CD3 stimulation. Mean percentages ± SE are shown.

Otherwise, MHV-JHM infection produced a cytokine mRNA profile distinct from that following MHV-A59 infection. Most striking was the difference in the induction of IFNβ and IFNγ mRNA levels. IFNβ message was induced early in MHV-JHM infection, before the infiltration of peripheral immune cells, and continuously transcribed into day 7, after the arrival of peripheral immune cells (Fig. 2). This differed from MHV-A59 infection where moderate IFNβ mRNA accumulation evident at day 3 was further reduced by day 7. In contrast to its ability to induce IFNβ, IL-12 p40 and IFNγ messages were not detected until 5 days after MHV-JHM infection, but were already evident 3 days following MHV-A59 infection (Fig. 2). These differences in interferon transcript levels could significantly influence the direct ability to clear MHV, as well as the infiltration of T cells into the brain (Yasuda et al., 1999; Zou et al., 1999).

MHV-JHM infection results in a diminished CD8 T cell presence in the CNS

The ability of MHV-JHM infection to influence T cell infiltration was evaluated. Following MHV infection, lymphocytes begin to enter the brain about day 5 with their numbers peaking at about day 7 when virus-specific cytolytic CD8 T cells are apparent (Castro et al., 1994; Marten et al., 2001). Therefore, mononuclear cells were isolated from infected brains on day 7 and stained to distinguish CD8, CD4, and NK1.1 cells. MHV-JHM-infected brains yielded approximately a 2.5-fold decrease in the percentage of CD8 T cells within the infiltrating cell population as compared to MHV-A59-infected brains. The lack of a difference in the percentage of CD4 T cells and NK T cells within the brains suggested that they contributed less than CD8 T cells to the observed differences in pathology (Fig. 3).

Unlike IFNβ, IFNγ is critical in MHV clearance (Marten et al., 2001; Parra et al., 1999; Schijns et al., 1998). Thus, the capacity of CD8 T cells to produce IFNγ was also examined by intracellular staining. Mononuclear cells isolated from infected brains were stimulated with a control peptide or viral peptides (S510 or S598). Whether other epitopes exist on the MHV-A59 background is currently unknown (Marten et al., 2001). As previously demonstrated (Castro et al., 1994), the S510 epitope was immunodominant in MHV-JHM infection (Fig. 4A). CD8 cells from MHV-JHM-infected brains also exhibited a greater response against the S598 epitope compared to cells from MHV-A59-infected brains (Fig. 4B). Anti-CD3 activates antigen-experienced cells (Yee et al., 1994) and was used to characterize the ability of total CD8 T cell population, which entered the brain in response to infection, to produce IFNγ. To evaluate the relationship between the anti-CD3 and viral peptide stimulations, the percentages of IFNγ+ CD8 T cells observed following these stimulations were compared (Fig. 4C). MHV-JHM infection resulted in similar percentages of IFNγ+ CD8 T cells in response to either anti-CD3 (21.5%) or known viral peptides (24.2%), resulting in a viral/anti-CD3 ratio of 1:1. In contrast, following MHV-A59 infection, only about 0.29 of the anti-CD3 response reflected that of the viral peptide S598.

Furthermore, the reduced number of CD8 T cells in the brain following MHV-JHM infection decreased the potential for IFNγ production within the CNS. When the percentage of IFNγ+ cells within the intact mononuclear gate was assessed, there was about a 3-fold lower percentage of IFNγ+ cells from MHV-JHM, as compared to MHV-A59, infected brain (Fig. 4D).

The diminished CD8 T cell presence in MHV-JHM-infected brains may reflect a microenvironment that does not augment CD8 T cell infiltration into the CNS. Alterna-

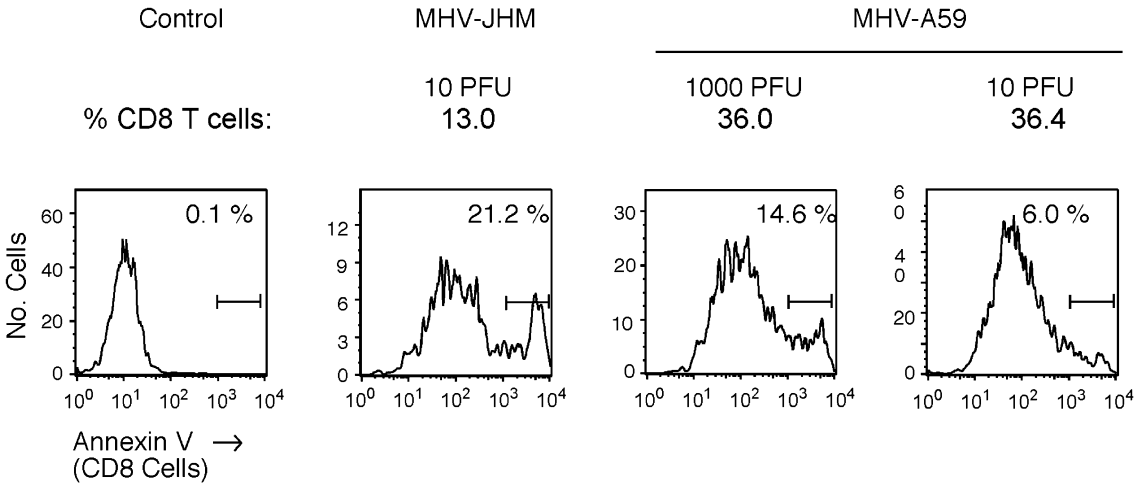

Fig. 5. Enhanced CD8 T cell apoptosis is seen following MHV-JHM infection. Cells isolated from infected brains were stained with anti-CD8 and Annexin V. Histograms shown were gated on CD8-positive cells. Control panel represents cell sample (from MHV-JHM-infected brains) in the absence of Annexin V staining. One representative experiment of three is shown. The intensity of Annexin V staining of negative population from control to sample is consistent with the assay parameters of the manufacturer.

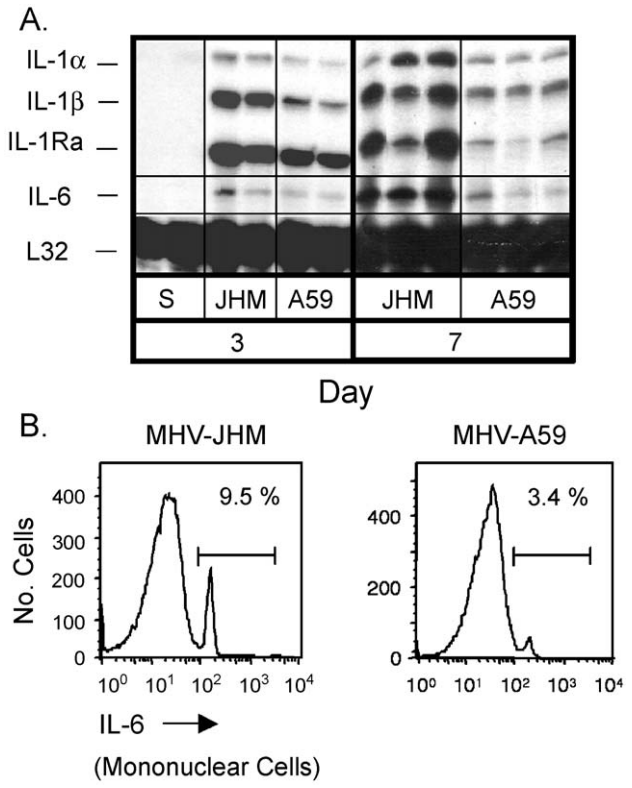

Fig. 6. Fatal encephalitis is associated with elevated IL-6 synthesis. (A) Mice were infected intracranially with MHV-JHM or MHV-A59. On days 3, 5, and 7 p.i., animals were perfused and brains were harvested. Total RNA was extracted and analyzed by RPA. Representative samples shown from four experiments. (B) Cells were isolated from infected brains on day 7. Cells were incubated in the presence of UV-irradiated virus and monensin for 5 h at 37 °C, then stained for intracellular IL-6 as described in Materials and Methods. Experiment was repeated with similar results.

tively, or in addition, this microenvironment may support enhanced CD8 T cell apoptosis (Fig. 5). This possibility was examined by staining cells isolated from MHV-JHM- and MHV-A59-infected brains with anti-CD8 and Annexin V. In three independent experiments, CD8 T cells from MHV-JHM-infected brains exhibited enhanced apoptosis compared to CD8 T cells from MHV-A59-infected brains (18.0 ± 1.7 vs. 10.7 ± 2.1; $P < 0.05$).

MHV-JHM infection induces elevated IL-1 and IL-6 transcripts

Relative to MHV-A59, MHV-JHM infection yielded greater IL-1α and IL-1β mRNA accumulation, evident as early as day 3 and continuing through to day 7 (Fig. 6A). IL-1 is considered a key IL-6 inducer within the CNS (Gottschall et al., 1994) consistent with the increasing strength of IL-6 mRNA levels from day 3 to day 7 following MHV-JHM infection (Fig. 6A). In contrast, MHV-A59 inoculation resulted in moderate IL-6 mRNA accumulation. The observed disparity in IL-6 mRNA expression was confirmed by intracellular staining for IL-6 (Fig. 6B). Mononuclear cells isolated from MHV-JHM-infected mice resulted in a 3-fold increase in the percentage of IL-6-positive cells as compared to those from MHV-A59-infected mice. Moreover, supernatants of mixed glial neuronal cultures infected with MHV-JHM had enhanced IL-6 production as compared to MHV-A59 (Rempel et al., 2004). Therefore, MHV-JHM infection induced aberrant levels of IL-6.

MHV-JHM infection is associated with enhanced macrophage infiltration

MHV-JHM-infected brains exhibited elevated levels of MIP-1α, MIP-1β, and MIP-2 mRNA as early as day 3 and through to day 7 (Fig. 7). This suggested that a greater recruitment of macrophages into the brain could be initiated early in MHV-JHM infection. This possibility was evaluated directly by FACS analysis of cells within the analyzed within the mononuclear cell gate (as determined by forward and side scatter) and stained with macrophage markers. Macrophage populations were determined by staining isolated cells with anti-CD45 and either anti-FcγR or anti-CD11b enabling differentiation between macrophages

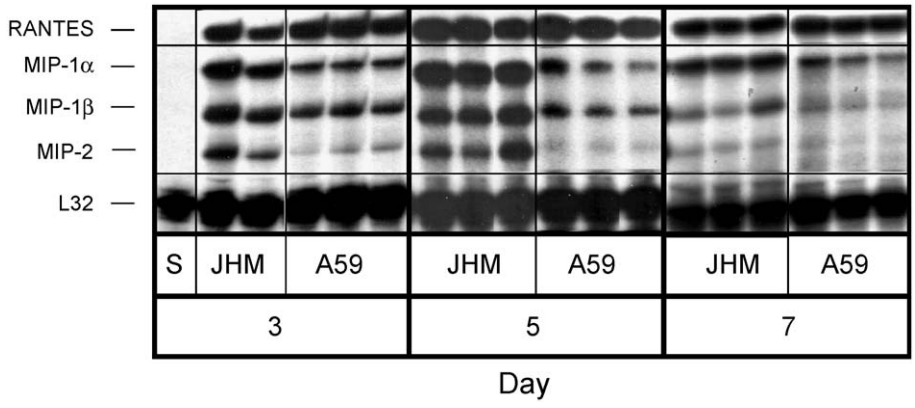

Fig. 7. MIP-1α, MIP-1β, and MIP-2 mRNA levels are enhanced in MHV-JHM-infected brains. Mice were infected with MHV-A59 or MHV-JHM as stated for Fig. 2. Total RNA was isolated from brains and analyzed by RPA. Representative samples shown from four experiments.

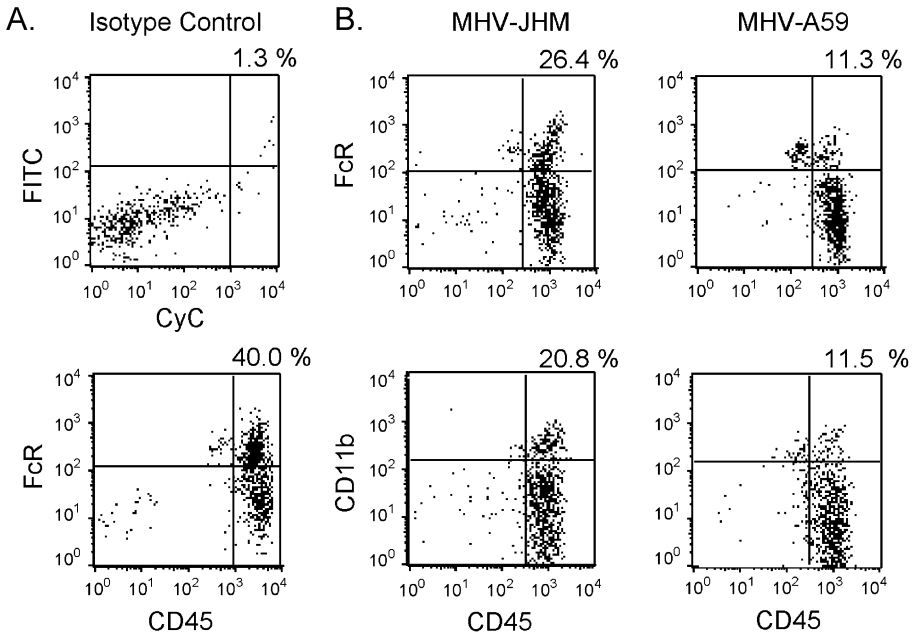

Fig. 8. MHV-JHM infection results in a greater infiltration of macrophages into the brain. (A) Isotype controls reflect percentages from one representative experiment (MHV-JHM samples). (B) Cells isolated from MHV-JHM- or MHV-A59-infected brains on day 7 were stained for either CD45 and FcR or CD45 and CD11b. Percentages above quadrants reflect the percentage of cells within the upper right-hand quadrant, that is, either CD45 high/FcR high or CD45 high/CD11b high. One representative experiment. (C) Means ± SE for *N* experiments is shown.

(CD45 high/CD11b high) and microglial cells (CD45 intermediate/CD11b high) (Carson et al., 1998). MHV-JHM-infected brains demonstrated approximately 2-fold greater percentages of macrophages defined as either CD45 high/FcγR high or CD45 high/CD11b high phenotypes (Fig. 8). B220 staining was more intense following MHV-A59 infection (data not shown), indicating that disparity in CD45 high/FcγR high staining was not due to greater numbers of B cells in MHV-JHM-infected brains. Thus, strong macrophage responses were clearly not protective, but were associated with severe viral encephalitis.

Discussion

The results presented in this report provide a framework to interpret the biological basis for the extraordinary neurovirulence of MHV-JHM. It is apparent that a key decisive event in the pathogenesis of MHV-JHM is the early activation of innate immune responses reflected by elevated and sustained activation of IFNβ and IL-6, together with the accumulation of MIP-1α, MIP-1β, and MIP-2 mRNA. A subsequent impact on leukocyte recruitment was evident by the macrophage-dominated cellular infiltrate deficient in CD8 T cells. This response, and the fatal consequence of MHV-JHM infection, stood in marked contrast to MHV-A59 infection where the enhanced induction of IFNγ transcripts supported CD8 T cell activity.

Early innate immunity is critical in the first line defense against viral infections, as well as in directing the development of protective adaptive responses. In this study, glial cell innate immune responses were evaluated at 3 days after intracranial inoculation, before peripheral mononuclear cell infiltration, by ribonuclease protection assay (RPA) analysis of whole brain samples (Marten et al., 2001). At this time, MHV-JHM and MHV-A59 induced distinct patterns of cytokine (Figs. 2 and 6) and chemokine (Fig. 7) transcripts. The RNA profiles of the two infections in vivo became increasingly divergent over time, corresponding to the infiltration of discrete leukocyte populations, suggesting that the polarization of leukocyte responses emerged out of virally induced innate CNS immunity and reinforced them.

Throughout the course of MHV-JHM and MHV-A59 infections, mRNA levels of MIF and TNFα were greatly enhanced (Fig. 2). Both infections also triggered the accumulation of early IFNβ transcripts that were sustained in MHV-JHM infection, but essentially undetectable in MHV-A59 infection by day 7, perhaps due to the difference in viral loads (Fig. 2). IFNβ production is an essential component in the control of some viral infections (Biron et al.,

1999; Orange and Biron, 1996). However, in MHV infection, continued IFNβ appears to have limited benefit, considering the strong, but clearly ineffective, IFNβ transcription seen in MHV-JHM infection (Fig. 2) and the inability of exogenous IFNβ to protect against MHV infection of astrocytoma cells (unpublished data). In contrast, IFNγ is considered essential for MHV clearance as observed by an increase in mortality among IFNγ-knockout and IFNγ receptor-knockout mice infected with attenuated MHV strains (Marten et al., 2001; Parra et al., 1999; Schijns et al., 1998). Interferons also impact T cell responses. The enhanced presence of IFNβ might impede T cell activity as demonstrated in experimental models of MS, where IFNβ treatment ameliorated disease impairing T cell proliferation and migration into the brain (Yasuda et al., 1999; Zou et al., 1999). IFNγ, on the other hand, promotes the T cell migration into the brain in part by upregulating adhesion and co-stimulatory molecules within the CNS and the periphery (Grau et al., 1997). Therefore, the lag in IFNγ mRNA expression and the enhanced IFNβ, compared to IFNγ, transcript levels following MHV-JHM inoculation (Fig. 2) could be instrumental to the failure to control viral replication both directly and indirectly resulting in the lack of appropriate support for CD8 T cells (Figs. 3, 4, and 5). The early (d. 3) resident brain cell, possibly neuronal, transcription of IFNγ mRNA in MHV-A59 infection defines an environment that would be more supportive of CD8 T cell responses (Mori et al., 2001).

Due to the established importance of CD8 T cells and IFNγ in the control of MHV infection, the capacity of CD8 T cells to produce IFNγ in response to the known viral epitopes was evaluated. Anti-CD3 stimulation was used as a positive control and to quantitate the capacity of the total CD8 T cell population to produce IFNγ. In MHV-JHM infection, the known viral epitopes reflected the full potential for antigen-experienced cells to produce IFNγ following anti-CD3 stimulation (indicating that in MHV-JHM infection, the response from the anti-CD3 stimulation is representative of the viral epitope stimulations, Fig. 4C). In contrast, following MHV-A59 infection, the viral epitope stimulations were a fraction (0.29) of the anti-CD3 stimulation. This suggests that an undefined immunodominant epitope, capable of inducing IFNγ synthesis, exists within the MHV-A59 genome that is absent in MHV-JHM. Alternatively, this may reflect the activation of non-virus-specific CD8 cells or some combination of these events (Bergmann et al., 1999). The diminished CD8 T cell presence in MHV-JHM-infected brains also appeared to reduce the potential for IFNγ production in the brain, resulting in a 3-fold lower potential percentage of IFNγ+ mononuclear cells isolated from the MHV-JHM-infected brain as compared to MHV-A59-infected brain (Fig. 4D).

The differences in the CD8 T cell presence in the brain following MHV-JHM and MHV-A59 infections were associated with increased CD8 cell apoptosis in MHV-JHM infection (Fig. 5). The enhanced CD8 apoptosis may reflect clonal exhaustion of anti-viral CD8 T cells due to the high antigenic burden of elevated MHV-JHM titers (Moskophidis et al., 1993). Alternatively, macrophages recruited into the brain upon MHV-JHM infection (Fig. 8) may instigate or amplify CD8 T cell apoptosis, as activated macrophages can induce premature CD8 T cell apoptosis (Bronte et al., 1998). Moreover, enhanced T cell apoptosis was observed within a week of a lethal influenza viral strain HK483 concomitant with elevated MIP-1α production within the brain (Tumpey et al., 2000). Further studies should determine whether macrophage activity influences CD8 T cell survival in MHV-JHM infection.

Importantly, the failure of MHV-JHM infection to induce protective T cell responses did not reflect a generalized immune suppression. On the contrary, robust transcription of IL-1 and IL-6 mRNA following MHV-JHM, but not MHV-A59, infection was evident (Fig. 6). The ability of MHV-JHM to induce greater production of IL-6 protein was confirmed by intracellular cytokine staining of cells isolated from the brain (Fig. 6B) and in vitro within the supernatant of mixed glial neuronal cultures (Rempel et al., 2004). Chronic IL-6 production has been implicated in CNS inflammatory diseases including experimental autoimmune encephalomyelitis (Merrill, 1992; Okuda et al., 1999; Sun et al., 1995; Vandenabeele and Fiers, 1991). High levels of IL-6 transcripts, in the presence of either IFNβ or IL-1 message, have also been documented in lethal encephalitic viral infections (Parra et al., 1997; Theil et al., 2000; Wesselingh et al., 1994). Astrocytes are a main reservoir for MHV within the CNS and previously have been shown to be a primary producer of IL-6 following MHV infection (Sun et al., 1995). Negligible FACS co-staining of IL-6 with CD8 or CD11b (data not shown) supported the probability that astrocytes were the source of the IL-6 observed here. The contribution of MHV-JHM-induced IL-6 production to CNS responses is the subject of an ongoing investigation using mixed glial neuronal cultures.

MHV-JHM infection induced elevated levels of MIP-1α, MIP-1β, and MIP-2 transcripts by glial cells (day 3 p.i.) compared to MHV-A59 (Fig. 7). Activated glial cells can produce chemokines thereby influencing the composition of the ensuing cellular infiltrate. In vitro and in vivo studies have demonstrated that glial cells produce MIP-1α and MIP-1β, along with RANTES, in response to MHV and other CNS infections (Asensio et al., 1999; Hoffman et al., 1999; Kitai et al., 2000; Lane et al., 1998). MIP-1α and MIP-1β predominately enhanced the migration of macrophages, eosinophils, and T cells (Baggiolini et al., 1994). Upregulation of MIP-1 message following MHV-JHM infection corresponded with elevated CD45 high/FcR high or CD45 high/CD11b high staining positive cells assessed within a mononuclear cell gate (Carson et al., 1998). These cells are most likely macrophages as staining with anti-B220 and anti-NK1.1 was, respectively, diminished and similar from MHV-JHM compared to MHV-A59-infected brains (data not shown, Fig. 3). Although macrophages

often play a protective role in immune defense, their presence has also been associated with inflammatory diseases, lethal viral infections, and neurodegeneration (Lidbury et al., 2000; Smits et al., 2000; Xiong et al., 1999). Severe MHV infections have been previously associated with increased macrophage activation, seen in the upregulation of inducible nitric oxide synthase message in the brain and macrophage procoagulant activity in the periphery (Fingerote et al., 1996; Parra et al., 1997). It is probable that the heightened MIP-2 mRNA levels that were observed in MHV-JHM infection are chemotatic for neutrophils. Preliminary experiments with anti-Ly-6G monoclonal antibody (RB6, using a polynuclear cell gate) revealed a 1.6- to 2-fold greater presence of neutrophils in MHV-JHM-infected brains as compared to MHV-A59 (data not shown). Future studies may demonstrate that neutrophils contribute to the limited protection seen in wild-type MHV-JHM infection, as observed in broader protection seen following an attenuated MHV-JHM viral infection (Zhou et al., 2003). However, taken together, the chemokine and cellular infiltration patterns observed here support our conclusion that MHV-JHM infection induces a pattern of immune responses that may be detrimental to recovery.

Understanding how a virus, especially one as complex as MHV, manipulates the host immune response and the resulting disease is a daunting endeavor and requires consideration of both viral genetics and host responses. An increasing number of viral components have been found to activate different immune responses, including IFNγ down-regulation and apoptosis (Basler et al., 2000; Chen et al., 2001; Park et al., 2001). Considering the genetic similarity of MHV-JHM and MHV-A59, it is likely that distinct viral gene products will be found to impact immune responses. Zhang et al. (1998) reported that expression of MHV-JHM hemagglutinin/esterase, using defective interfering particles, in a MHV-A59 infection enhances the accumulation of IL-6 mRNA in vitro. In addition, other studies in our laboratory (submitted) indicate that elevated MIP-1 transcripts and macrophage recruitment by MHV-JHM was associated with enhanced mortality following infection with a chimeric virus containing the MHV-JHM spike gene expressed on the MHV-A59 background.

Our study, as well as those by others, provides clues to understanding how viruses manipulate the immune response to CNS infection, thereby altering the course of disease. It is hoped that these investigations will provide insight into potential therapeutic avenues for treatment of viral encephalitis and demyelination.

Materials and Methods

Mice and viruses

Age-matched (5–6 weeks old) male C57Bl/6 mice were infected intracranially with 30 μl of MHV-JHM (also known as MHV-4, LD50 3 PFU) at 10 PFU (Phillips et al., 1999) while under methoxyflurane anesthesia (Pitman-Moore Inc., Washington Crossing, NJ), the following control inoculations were given: diluent or MHV-A59 (LD50 4680 PFU). MHV-A59 results in mild encephalitis at 10 PFU (Phillips et al., 1999; Talbot and Buchmeier, 1985). Therefore, MHV-A59 was also administered at 1000 PFU, a dose that produces similar disease scores as MHV-JHM on day 7, the peak of encephalitis (Fig. 1). Day 7 was used as an end point, since mice infected with MHV-JHM generally succumbed to infection between days 7 and 10. On days 3, 5, and 7, animals were anesthetized with chloral hydrate (Sigma, St. Louis, MO) and perfused with saline. The brains were removed, and halves were used for either plaque assays or RNA isolation. In other experiments, cells were harvested from the brains of infected mice to assess extracellular surface markers and intracellular cytokine staining by FACS analysis.

Clinical disease

Clinical disease provided an external reference for the degree of encephalitis. Clinical disease was scored on day 7 as disease signs were not consistently evident at day 5. Briefly, disease scores ranged as follows: 0, no clinical signs; 1, ruffled hair; 2 ruffled hair, hunched back and slight impairment in mobility; 3, ruffled hair, hunched back and extreme impairment of mobility; and 4, mortality.

Mononuclear cell isolation from the brain

Mononuclear cells were isolated from perfused brains as previously described (Haring et al., 2001). Four to six mice per group were used in each experiment. Briefly, brains were removed and placed in Petri dishes containing media consisting of RPMI (GibcoBRL, Grand Island, NY) and 10% fetal calf serum (FCS, HyClone, Logan, UT). To obtain single cell suspensions, brains were ground between frosted slides and triturated with a wide bore pipette. Cell suspensions were transferred to 15-ml conical tubes containing 90% percoll (Amersham Pharmacia, Piscataway, NJ) resulting in a final percoll concentration of 30%. The suspensions were spun at 320 × *g* for 30 min at 4 °C. The lipids and supernatant were decanted. The remaining cells were pooled within a group, washed with media, underlayed with Lympholyte M (Cedarlane, Hornby, ON), and centrifuged at 1000 × *g* for 20 min at room temperature. The interface was collected and washed with media. Total viable cells were counted by trypan blue exclusion and the number of cells per brain was estimated. Approximately 450 000 cells per brain were isolated per group (Fig. 1).

Flow cytometry

All staining reagents were acquired from BD Biosciences Pharmingen, San Diego, CA. Isolated cells were used

at about 250 000 cells per tube and analyzed within the mononuclear cell gate as determined by forward and side scatter. T cells were detected by Cy-Chrome (CyC)-conjugated rat anti-mouse CD8a (clone 53-6.7) and *R*-phycoerytrin (PE)-anti-CD4 (clone H129.19) staining. NK cells were identified with PE-anti-NK1.1 (clone PK136). FITC-conjugated Annexin V was used to detect apoptotic CD8 T cells according to manufacturer's instructions. To identify macrophage populations, cells were stained with CyC-anti-CD45 (clone 30F11) and fluorescein isothiocyanate (FITC)-conjugated rat anti-mouse FcR (clone 2.4G2) or PE-conjugated CD11b (clone M1/70).

The potential of CD8 T cells to produce IFNγ was evaluated by intracellular cytokine staining (Haring et al., 2001). Isolated cells were incubated for 5 h at 37 °C in 10% FCS–RPMI containing brefeldin A in the presence of viral peptides specific for known CD8 epitopes, spike glycoprotein S510-518 or S598-605 (1 μM), or anti-CD3 (10 μg/ml). IFNγ was detected with FITC-anti-IFNγ (clone XMG1.2). The percentage of mononuclear cells staining for intracellular IL-6 was determined. Cells were stimulated with media or UV-irradiated virus in the presence of monensin for 5 h at 37 °C and stained with PE-conjugated anti-IL-6 (clone MP5-20F3) as described (Saio et al., 2001; Schuerwegh et al., 2001). The percentage of T cells and macrophages were estimated using a mononuclear gate. All gates were verified by back-gating to the forward or side scatter plot. Stained cells were collected on FASCScan (Becton Dickinson, Franklin Lakes, NJ) and analyzed with CellQuest software (BD Biosciences Pharmingen).

Ribonuclease protection assay

Total RNA was extracted from the brains of sham and MHV inoculated mice on days 3, 5, and 7 post infection using TRIzol reagent (GibcoBRL). Cytokine and chemokine RNA messages were quantified by RPA (Stalder and Campbell, 1994). Templates (BD PharMingen) were labeled with UTP-P^{32} (Amersham Pharmacia). Signal intensity was determined from scanned autoradiographs using the NIH Image 1.61 software. Target bands were normalized against the ribosomal subunit L32 RNA.

Acknowledgments

This research was supported by NIH Grants AI-43103, AI-25913, MH-62261, and P30MH62261. Dr. J.D. Rempel was a recipient of Multiple Sclerosis Society of Canada and National Multiple Sclerosis Society (U.S.) fellowships.

The authors would like to thank Drs. Howard Fox, Dan Hassett, and Ben Newman for critical reading of the manuscript and Ms. Phyllis Minick for editorial assistance.

References

Asensio, V.C., Kincaid, C., Campbell, I.L., 1999. Chemokines and the inflammatory response to viral infection in the central nervous system with a focus on lymphocytic choriomeningitis virus. J. NeuroVirol. 5, 65–75.

Baggiolini, M., Dewald, B., Moser, B., 1994. Interleukin-8 and related chemotactic cytokines—CXC and CC chemokines. Adv. Immunol. 55, 97–179.

Basler, C.F., Wang, X., Muhlberger, E., Volchkov, V., Paragas, J., Klenk, H.D., Garcia-Sastre, A., Palese, P., 2000. The Ebola virus VP35 protein functions as a type I IFN antagonist. Proc. Natl. Acad. Sci. U.S.A. 97, 12289–12294.

Bergmann, C.C., Yao, Q., Lin, M., Stohlman, S.A., 1996. The JHM strain of mouse hepatitis virus induces a spike protein-specific Db-restricted cytotoxic T cell response. J. Gen. Virol. 77, 315–425.

Bergmann, C.C., Altman, J.D., Hinton, D., Stohlman, S.A., 1999. Inverted immunodominance and impaired cytolytic function of CD8+ T cells during viral persistence in the central nervous system. J. Immunol. 163, 3379–3387.

Biron, C.A., Nguyen, K.B., Pien, G.C., Cousens, L.P., Salazar-Mather, T.P., 1999. Natural killer cells in antiviral defense: function and regulation by innate cytokines. Annu. Rev. Immunol. 17, 189–220.

Bronte, V., Wang, M., Overwijk, W.W., Surman, D.R., Pericle, F., Rosenberg, S.A., Restifo, N.P., 1998. Apoptotic death of CD8+ T lymphocytes after immunization: induction of a suppressive population of Mac-1+/Gr-1+ cells. J. Immunol. 161, 5313–5320.

Carson, M.J., Reilly, C.R., Sutcliffe, J.G., Lo, D., 1998. Mature microglia resemble immature antigen-presenting cells. Glia 22, 72–85.

Castro, R.F., Perlman, S., 1996. Differential antigen recognition by T cells from the spleen and central nervous system of coronavirus-infected mice. Virology 222, 247–251.

Castro, R.F., Evans, G.D., Jaszewski, A., Perlman, S., 1994. Coronavirus-induced demyelination occurs in the presence of virus-specific cytotoxic T cells. Virology 200, 733–743.

Chen, W., Calvo, P.A., Malide, D., Gibbs, J., Schubert, U., Bacik, I., Basta, S., O'Neill, R., Schickli, J., Palese, P., Henklein, P., Bennink, J.R., Yewdell, J.W., 2001. A novel influenza A virus mitochondrial protein that induces cell death. Nat. Med. 7, 1306–1312.

Fingerote, R.J., Abecassis, M., Phillips, M.J., Rao, Y.S., Cole, E.H., Leibowitz, J., Levy, G.A., 1996. Loss of resistance to murine hepatitis virus strain 3 infection after treatment with corticosteroids is associated with induction of macrophage procoagulant activity. J. Virol. 70, 4275–4282.

Gombold, J.L., Sutherland, R.M., Lavi, E., Paterson, Y., Weiss, S.R., 1995. Mouse hepatitis virus A59-induced demyelination can occur in the absence of CD8+ T cells. Microb. Pathog. 18, 211–221.

Gottschall, P.E., Tatsuno, I., Arimura, A., 1994. Regulation of interleukin-6 (IL-6) secretion in primary cultured rat astrocytes: synergism of interleukin-1 (IL-1) and pituitary adenylate cyclase activating polypeptide (PACAP). Brain Res. 637, 197–203.

Grau, V., Herbst, B., van der Meide, P.H., Steiniger, B., 1997. Activation of microglial and endothelial cells in the rat brain after treatment with interferon-gamma in vivo. Glia 19, 181–189.

Haring, J.S., Pewe, L.L., Perlman, S., 2001. High-magnitude, virus-specific CD4 T-cell response in the central nervous system of coronavirus-infected mice. J. Virol. 75, 3043–3047.

Hoffman, L.M., Fife, B.T., Begolka, W.S., Miller, S.D., Karpus, W.J., 1999. Central nervous system chemokine expression during Theiler's virus-induced demyelinating disease. J. NeuroVirol. 5, 635–642.

Kitai, R., Zhao, M.L., Zhang, N., Hua, L.L., Lee, S.C., 2000. Role of MIP-1beta and RANTES in HIV-1 infection of microglia: inhibition of infection and induction by IFNbeta. J. Neuroimmunol. 110, 230–239.

Lai, M.M., Stohlman, S.A., 1981. Comparative analysis of RNA genomes of mouse hepatitis viruses. J. Virol. 38, 661–670.

Lane, T.E., Asensio, V.C., Yu, N., Paoletti, A.D., Campbell, I.L.,

Buchmeier, M.J., 1998. Dynamic regulation of alpha− and beta-chemokine expression in the central nervous system during mouse hepatitis virus-induced demyelinating disease. J. Immunol. 160, 970–978.

Lavi, E., Gilden, D.H., Highkin, M.K., Weiss, S.R., 1984. Persistence of mouse hepatitis virus A59 RNA in a slow virus demyelinating infection in mice as detected by in situ hybridization. J. Virol. 51, 563–566.

Lavi, E., Das Sarma, J., Weiss, S.R., 1999. Cellular reservoirs for coronavirus infection of the brain in beta2-microglobulin knockout mice. Pathobiology 67, 75–83.

LeBlanc, R.A., Pesnicak, L., Cabral, E.S., Godleski, M., Straus, S.E., 1999. Lack of interleukin-6 (IL-6) enhances susceptibility to infection but does not alter latency or reactivation of herpes simplex virus type 1 in IL-6 knockout mice. J. Virol. 73, 8145–8151.

Lidbury, B.A., Simeonovic, C., Maxwell, G.E., Marshall, I.D., Hapel, A.J., 2000. Macrophage-induced muscle pathology results in morbidity and mortality for Ross River virus-infected mice. J. Infect. Dis. 181, 27–34.

Liu, M.T., Lane, T.E., 2001. Chemokine expression and viral infection of the central nervous system: regulation of host defense and neuropathology. Immunol. Res. 24, 111–119.

Marten, N.W., Stohlman, S.A., Bergmann, C.C., 2001. MHV infection of the CNS: mechanisms of immune-mediated control. Viral Immunol. 14, 1–18.

Merrill, J.E., 1992. Proinflammatory and antiinflammatory cytokines in multiple sclerosis and central nervous system acquired immunodeficiency syndrome. J. Immunother. 12, 167–170.

Mori, I., Hossain, M.J., Takeda, K., Okamura, H., Imai, Y., Kohsaka, S., Kimura, Y., 2001. Impaired microglial activation in the brain of IL-18-gene-disrupted mice after neurovirulent influenza a virus infection. Virology 287, 163–170.

Moskophidis, D., Lechner, F., Pircher, H., Zinkernagel, R.M., 1993. Virus persistence in acutely infected immunocompetent mice by exhaustion of antiviral cytotoxic effector T cells. Nature 362, 758–761.

Noseworthy, J.H., 1999. Progress in determining the causes and treatment of multiple sclerosis. Nature 399, A40–A47.

Okuda, Y., Sakoda, S., Fujimura, H., Saeki, Y., Kishimoto, T., Yanagihara, T., 1999. IL-6 plays a crucial role in the induction phase of myelin oligodendrocyte glucoprotein 35–55 induced experimental autoimmune encephalomyelitis. J. Neuroimmunol. 101, 188–196.

Olsson, T., 1995. Critical influences of the cytokine orchestration on the outcome of myelin antigen-specific T-cell autoimmunity in experimental autoimmune encephalomyelitis and multiple sclerosis. Immunol. Rev. 144, 245–268.

Olson, J.K., Girvin, A.M., Miller, S.D., 2001. Direct activation of innate and antigen-presenting functions of microglia following infection with Theiler's virus. J. Virol. 75, 9780–9789.

Orange, J.S., Biron, C.A., 1996. An absolute and restricted requirement for IL-12 in natural killer cell IFN-gamma production and antiviral defense. Studies of natural killer and T cell responses in contrasting viral infections. J. Immunol. 156, 1138–1142.

Park, I.W., Ullrich, C.K., Schoenberger, E., Ganju, R.K., Groopman, J.E., 2001. Hiv-1 tat induces microvascular endothelial apoptosis through caspase activation. J. Immunol. 167, 2766–2771.

Parra, B., Hinton, D.R., Lin, M.T., Cua, D.J., Stohlman, S.A., 1997. Kinetics of cytokine mRNA expression in the central nervous system following lethal and nonlethal coronavirus-induced acute encephalomyelitis. Virology 233, 260–270.

Parra, B., Hinton, D.R., Marten, N.W., Bergmann, C.C., Lin, M.T., Yang, C.S., Stohlman, S.A., 1999. IFN-gamma is required for viral clearance from central nervous system oligodendroglia. J. Immunol. 162, 1641–1647.

Pavesi, G., Gemignani, F., Macaluso, G.M., Ventrua, P., Magnani, G., Fiocchi, A., Medici, D., Marbini, A., Mancia, D., 1992. Acute sensory and autonomic neuropathy: possible association with coxsackie B virus infection. J. Neurol., Neurosurg. Psychiatry 55, 613–615.

Phillips, J.J., Chua, M.M., Lavi, E., Weiss, S.R., 1999. Pathogenesis of chimeric MHV4/MHV-A59 recombinant viruses: the murine coronavirus spike protein is a major determinant of neurovirulence. J. Virol. 73, 7752–7760.

Phillips, J.J., Chua, M.M., Rall, G.F., Weiss, S.R., 2002. Murine coronavirus spike glycoprotein mediates degree of viral spread, inflammation, and virus-induced immunopathology in the central nervous system. Virology 301, 109–120.

Rempel, J.D., Murray, S.J., Meisner, J., Buchmeier, M.J., 2004. Mouse hepatitis virus neurovirulence: evidence of a linkage between S glycoprotein expression and immunopathology. Virology 318, 45–54.

Saio, M., Radoja, S., Marino, M., Frey, A.B., 2001. Tumor-infiltrating macrophages induce apoptosis in activated CD8(+) T cells by a mechanism requiring cell contact and mediated by both the cell-associated form of TNF and nitric oxide. J. Immunol. 167, 5583–5593.

Schijns, V.E., Haagmans, B.L., Wierda, C.M., Kruithof, B., Heijnen, I.A., Alber, G., Horzinek, M.C., 1998. Mice lacking IL-12 develop polarized Th1 cells during viral infection. J. Immunol. 160, 3958–3964.

Schuerwegh, A.J., Stevens, W.J., Bridts, C.H., De Clerck, L.S., 2001. Evaluation of monensin and brefeldin A for flow cytometric determination of interleukin-1 beta, interleukin-6, and tumor necrosis factor-alpha in monocytes. Cytometry 46, 172–176.

Shoji, H., Azuma, K., Nishimura, Y., Fujimoto, H., Sugita, Y., Eizuru, Y., 2002. Acute viral encephalitis: the recent progress. Intern. Med. 41, 420–428.

Smits, H.A., Boven, L.A., Pereira, C.F., Verhoef, J., Nottet, H.S., 2000. Role of macrophage activation in the pathogenesis of Alzheimer's disease and human immunodeficiency virus type 1-associated dementia. Eur. J. Clin. Invest. 30, 526–535.

Stalder, A.K., Campbell, I.L., 1994. Simultaneous analysis of multiple cytokine receptor mRNAs by RNase protection assay in LPS-induced endotoxemia. Lymphokine Cytokine Res. 13, 107–112.

Sun, N., Grzybicki, D., Castro, R.F., Murphy, S., Perlman, S., 1995. Activation of astrocytes in the spinal cord of mice chronically infected with a neurotropic coronavirus. Virology 213, 482–493.

Talbot, P.J., Buchmeier, M.J., 1985. Antigenic variation among murine coronaviruses: evidence for polymorphism on the peplomer glycoprotein, E2. Virus Res. 2, 317–328.

Theil, D.J., Tsunoda, I., Libbey, J.E., Derfuss, T.J., Fujinami, R.S., 2000. Alterations in cytokine but not chemokine mRNA expression during three distinct Theiler's virus infections. J. Neuroimmunol. 104, 22–30.

Tumpey, T.M., Lu, X., Morken, T., Zaki, S.R., Katz, J.M., 2000. Depletion of lymphocytes and diminished cytokine production in mice infected with a highly virulent influenza A (H5N1) virus isolated from humans. J. Virol. 74, 6105–6116.

van Berlo, M.F., Warringa, R., Wolswijk, G., Lopes-Cardozo, M., 1989. Vulnerability of rat and mouse brain cells to murine hepatitis virus (JHM-strain): studies in vivo and in vitro. Glia 2, 85–93.

Vandenabeele, P., Fiers, W., 1991. Is amyloidogenesis during Alzheimer's disease due to an IL-1-/IL-6-mediated 'acute phase response' in the brain? Immunol. Today 12, 217–219.

Wesselingh, S.L., Levine, B., Fox, R.J., Choi, S., Griffin, D.E., 1994. Intracerebral cytokine mRNA expression during fatal and nonfatal alphavirus encephalitis suggests a predominant type 2 T cell response. J. Immunol. 152, 1289–1297.

Woyciechowska, J.L., Trapp, B.D., Patrick, D.H., Shekarchi, I.C., Leinikki, P.O., Sever, J.L., Holmes, K.V., 1984. Acute and subacute demyelination induced by mouse hepatitis virus strain A59 in C3H mice. J. Exp. Pathol. 1, 295–306.

Xiong, H., Zheng, J., Thylin, M., Gendelman, H.E., 1999. Unraveling the mechanisms of neurotoxicity in HIV type 1-associated dementia: inhibition of neuronal synaptic transmission by macrophage secretory products. AIDS Res. Hum. Retroviruses 15, 57–63.

Yasuda, C.L., Al-Sabbagh, A., Oliveira, E.C., Diaz-Bardales, B.M., Garcia, A.A., Santos, L.M., 1999. Interferon beta modulates experimental autoimmune encephalomyelitis by altering the pattern of cytokine secretion. Immunol. Invest. 28, 115–126.

Yee, S.T., Kato, T., Tamura, T., Nariuchi, H., 1994. Different requirements of CD3 cross-linkage for the activation of memory and naive CD8+ T cells. Cell. Immunol. 157, 48–58.

Zhang, X., Hinton, D., Park, S., Liao, C.L., Lai, M.M., Stohlman, S., 1998. Using a defective-interfering RNA system to express the HE protein of mouse hepatitis virus for studying viral pathogenesis. Adv. Exp. Med. Biol. 440, 521–528.

Zhou, J., Stohlman, S.A., Hinton, D.R., Marten, N.W., 2003. Neutrophils promote mononuclear cell infiltration during viral-induced encephalitis. J. Immunol. 170, 3331–3336.

Zou, L.P., Ma, D.H., Wei, L., van der Meide, P.H., Mix, E., Zhu, J., 1999. IFN-beta suppresses experimental autoimmune neuritis in Lewis rats by inhibiting the migration of inflammatory cells into peripheral nervous tissue. J. Neurosci. Res. 56, 123–130.